JPPIPA 10(12) (2024)

Jurnal Penelitian Pendidikan IPA

Journal of Research in Science Education

http://jppipa.unram.ac.id/index.php/jppipa/index

Experimental and Theoretical Studies of Black Cumin Seed (*Nigella sativa*) Extract as Corrosion Inhibitor for ASTM A36 Steel

Yunia Maulida[1], Saprini Hamdiani[1], Sudirman[1], Saprizal Hadisaputra[2]*

[1] Department of Chemistry, Faculty of Mathematic and Natural Science, University of Mataram, Mataram, Indonesia.
[2] Chemistry Education Division, Faculty of Teacher Training and Education, University of Mataram, Mataram, Indonesia.

Received: July 18, 2024
Revised: October 31, 2024
Accepted: December 25, 2024
Published: December 31, 2024

Corresponding Author:
Saprizal Hadisaputra
rizal@unram.ac.id

DOI: 10.29303/jppipa.v10i12.8565

Abstract: Black cumin seed extract (*Nigella sativa*) is effective to control ASTM A36 steel corrosion in 1 M HCl solution. This study analyzed black cumin seed (BCS) extract as a corrosion inhibitor (0 to 500 ppm) by electrochemical method including Potentiodynamic Polarization (PDP) and Electrochemical Impedance Spectroscopy (EIS). The results revealed that with the PDP method the highest inhibition efficiency (IE) was 84.26% at the concentration of 500 ppm, and with the EIS method the IE value was 77.77% at the same concentration. The components of the extract were analyzed by GCMS and obtained major compounds are linoleic acid (22.12%), methyl linoleate (22.70%), 4-cyclopentene-1,3-dione,4-3-methyl-2-butenyl) (7.64%), methyl palmitate (6.66%), and palmitic acid (5.14%). A theoretical approach with computation was also carried out to investigate the performance and interaction of the major compounds in the BCS extract that a significant role as inhibitor. This was using Density Functional Theory (DFT) method and Monte Carlo simulation. The results showed that methyl linoleate compound as the most significant role.

Keywords: Black Cumin Seed (*Nigella sativa*); Corrosion Inhibitor; EIS; DFT; Monte Carlo; PDP

Introduction

ASTM A36 steel is one of the most easily corroded metals. Corrosion is damage due to chemical reactions between metals and their environment. ASTM A36 steel as a metal iron that is often used is very susceptible to corrosion because it is influenced by environmental factors that cam form rust Fe_2O_3 (Mulyati et al., 2019). On the other hand, the need for ASTM A36 iron continues to increase because it is a stronger and relatively cheap material. However, its weakness is that it is prone to corrosion over a period of time. Corrosion can result in large economic losses, especially in the industrial sector. The handling of this corrosion can reach 3-4% of the product budget (Prasad et al., 2020). Corrosion events cannot be prevented but the rate at which they occur can be reduced.

Reducing the corrosion rate is usually done by reducing metal contact with air (coating), cathodic plating, and with inhibitors. The use of coatings and cathodic coatings is less effective because it requires a relatively expensive cost. One method that is quite effective in reducing the corrosion rate is by using corrosion inhibitors (Hadisaputra et al., 2020). Based on Hassan et al. (2017), the use of tannin corrosion inhibitors on carbon steel has a slower corrosion rate of 0.0035 mm/year compared to the coating method with a corrosion rate of 0.09 mm/year. Therefore, the reduction of steel corrosion rate has now been widely done by using corrosion inhibitors.

In addition to reducing the corrosion rate, corrosion inhibitors are also easy to use, economical, and have high efficiency. Some corrosion inhibitors that are often used include surfactants and inorganic inhibitors. However, both of these inhibitors have disadvantages, they are not environmentally friendly because they are difficult to degrade and have high toxicity (Obot et al., 2019). The use of corrosion inhibitors that are environmentally friendly, cheap, and efficient is a solution, one of which is by using inhibitors from natural

How to Cite:
Maulida, Y., Hamdiani, S., Sudirman, S., & Hadisaputra, S. (2024). Experimental and Theoretical Studies of Black Cumin Seed (Nigella sativa) Extract as Corrosion Inhibitor for ASTM A36 Steel. *Jurnal Penelitian Pendidikan IPA*, *10*(12), 11170–11178. https://doi.org/10.29303/jppipa.v10i12.8565

materials. Hadisaputra et al. (2019) reported that the use of inhibitors natural materials can provide inhibition efficiency against iron corrosion. Compounds that can be used as corrosion inhibitors are that have heteroatoms and π bonds to interact with metals (Salarvand et al., 2017). Salam et al (2023) reported that citral compounds are one of the compounds that have heteroatoms and π bonds are very potential corrosion inhibitors against metal surfaces.

One of natural materials that has potential as a corrosion inhibitor is black cumin seeds (*Nigella sativa*). Black cumin seed (BCS) contain many heteroatomic compounds such as fatty acids, terpenoids, and quinone (Kabir et al., 2020). Proper extraction needs to be done to produce compounds that are thought a significant role as corrosion inhibitors (Hadisaputra et al., 2019). Extraction of BCS using methanol solvent produces greater yields than THF, DCM, petroleum ether and *n*-hexane solvents, with 34.8-47.95% using the soxhletation method (H. Kausar et al., 2018).

Experimental testing of corrosion inhibitor efficiency of natural material compounds has been widely carried out by electrochemical studies. This method excellent accuracy than conventional methods. Gapsari et al. (2024), showed that by using electrochemical methods, the corrosion rate and thermodynamic parameters (ΔH°_{Ads}, ΔS°_{Ads}, ΔG°_{Ads}) can be known to explain the adsorption that occurs in the corrosion process. The process and adsorption of corrosion inhibitor on metal surfaces can also be explained by theoretical studies using computational methods.

Theoretical studies of BCS extract on iron corrosion inhibition have not been conducted before. Therefore, theoretical studies also need to be carried out for molecular modeling with a computational method approach and to predict the compounds of the BCS extract that have the highest potential as corrosion inhibitors. Density Functional Theory (DFT) is usually widely used because it has a high level of accuracy in predicting the properties of molecules when compared to other methods. The interactions between organic inhibitors, corrosion agents and metal surfaces are also studied through Monte Carlo (MC) simulation. MC simulation can predict the adsorption energy to show the adsorption ability of the inhibitor on the iron surface (Hsissou et al., 2020).

Method

Extraction of Black Cumin Seeds

BCS were washed with distilled water and dried at room temperature (48 hours) and pulverized. BCS powder (100 g) was extracted by soxhletation method with methanol solvent (500 mL) for 6 hours. The solvent and extract were separated by rotary evaporator (40 °C) and the yield was calculated (H Kausar et al., 2018). Yield was calculated by the equation:

$$\text{Yield } (\%) = \frac{\text{Mass of extracted (g)}}{\text{Mass of raw material (g)}} \times 100 \qquad (1)$$

GC-MS Analysis

The methanol extract of BCS was analyzed by GC-MS (QP210 Ultra, Shimadzu). The identification of compound in the extract was based on the retention time of chromatogram peaks.

Specimen and Inhibitors Preparation

ASTM A36 steel was used in this test. The ASTM A36 used was made to a size 8 cm × 1 cm × 0.8 mm, with a test specimen area of 1 cm^2. The surface part instead of the test specimen in coated by epoxy resin. Before the specimen was subjected to corrosion test, the surface of the specimen was soothed with sandpaper grade 800 and 1500 then washed with distilled water and dried with tissue. Inhibitors were prepared with BCS extract at concentrations of 0, 100, 200, 300, 400, and 500 ppm (in 1 M HCl, v/v).

Electrochemical Measurement

Corrosion measurements were carried out at room temperature (298 K) using a Potentiostat Instrument (μStat-I 400s, Metrohm Drop Sens) with Drop View 8400 software control. Measurement was carried out in three electrode cells: platinum as counter electrode (CE), Ag/AgCl (3 M KCl) as reference electrode (RE), and ASTM A36 specimen as working electrode (WE). Before measurement, the specimens were immersed in the test solution (30 minutes) at Open Circuit Potential (OCP) to reach steady state.

Potentiodynamic Polarization (PDP) testing was carried out in the range of ± 250 mV vs. E_{corr} (Saleh et al., 2019). Calculation of inhibition efficiency (IE) is based on the equation:

$$IE_{PDP}\ (\%) = \frac{i_{corr} - i_{corr(i)}}{i_{corr}} \times 100 \qquad (2)$$

where i_{corr} dan $i_{corr(i)}$ represent corrosion current densities recorder under the uninhibited and inhibited conditions, respectively.

Meanwhile, Electrochemical Impedance Spectroscopy (EIS) testing was carried out with a frequency range of 100 kHz to 0.01 Hz with amplitude of 5 mV (Chellouli et al., 2016). Calculation of inhibition efficiency (IE) from EIS data is based on the equation:

$$IE_{EIS}(\%) = \frac{R_{ct(i)} - R_{ct}}{R_{ct(i)}} \times 100 \qquad (3)$$

where R_{ct} and $R_{ct(i)}$ are charge transfer resistance uninhibited and inhibited conditions, respectively.

Quantum Chemical Calculation

The determination of quantum parameters was carried out by the DFT B3LYP/31G(d) using Gaussian 0.9W dan Gauss View 6.0 software. The quantum chemical parameters determined were energy values of the highest occupied molecular orbital (E_{HOMO}) and the lowest unoccupied molecular orbital (E_{LUMO}), ΔE_{gab} (energy gab), ionization potential (IP), electron affinity (EA), electronegatifity (χ), hardness (η), softness (σ) and fraction of electrons transferred from the inhibitors to iron surface (ΔN).

$$IP = -E_{HOMO} \quad (4)$$

$$EA = -E_{LUMO} \quad (5)$$

$$\chi = \frac{IP + EA}{2} \quad (6)$$

$$\eta = \frac{IP - EA}{2} \quad (7)$$

$$\Delta N = \frac{\chi Fe - \chi inh}{2(\eta Fe + \eta inh)} \quad (8)$$

where χFe dan χinh indicate the absolute electronegativity values of iron metal and organic inhibitor, respectively, ηFe dan ηinh indicate the hardness values of iron and organic inhibitor. The values of χFe and ηFe are 4.82 and 0 (Lgaz et al., 2020).

Monte Carlo Simulations

MC simulation was performed using Material Studio 7.0 software. The simulation was implemented with Compass Force Field to optimize all inhibitor molecules (Hadisaputra et al., 2020). The inhibitor molecules were simulated on the Fe(110) metal surface with 20 × 20 supercells and 15 nm vacuum thickness created on the metal plane. Simulations were performed with atomic target on the Fe(110) surface using 1 inhibitors molecule and 100 H_2O molecules. The simulation yielded the adsorption energy of the inhibitor molecule on the Fe(110) surface.

Result and Discussion

Compound of Methanol Extract of BCS

BCS extracted with methanol solvent obtained an extract weight of 45.74 g in 100 g sample. The use of methanol solvent can extract BCS with a greater percent yield than other solvent. H. Kausar et al. (2018), reported that the extraction of BCS using methanol solvent produced greater yields than THF, DCM, petroleum ether and *n*-hexane, with 34,8-47,95% using the soxhletation method. The percent yield produced was 45,74%. These results are not much different from previous studies.

Characterization of the extraction results by GC-MS was carried out to detect compounds in the extract and determine the percentage of compounds quantitatively. Figure 1 shows the GC-MS chromatogram of methanol extract of BCS. Based on GC-MS analysis, the methanol extract of BCS contains fatty acid with the highest percentage. The highest percentage of linoleic acid in methanol extract of BCS is in accordance with previous studies. Alrashidi et al. (2020), in their research showed that methanol extract BCS contained 54.55% linoleic acid. Table 1 shows the percentage of compounds of BCS methanol extract with typical retention times.

Table 1. Major Compounds in Methanol Extract of BCS

Compounds	Rt	% Area	
		Results	Ref
Linoleic acid	12.688	25.12	54.55*
Methyl linoleate	12.496	22.70	1. 33**
4-Cyclopentene-1,3-dione,4-(3-methyl-2-butenyl)	9.161	7.64	0.95**
Methyl palmitate	11.896	6.66	0.08**
Palmitic acid	12.043	5.14	14.50*
Carvacrol	9.408	4.32	2.85**

Sources: *Alrashidi et al. (2020); **Kabir et al. (2020)

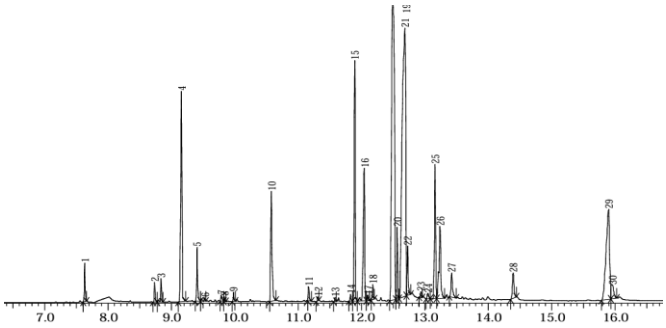

Figure 1. Profile GC-MS methanol extract of BCS

Potentiodynamic Polarization Curve

Potentiodynamic polarization (PDP) technique was used in the corrosion analysis of ASTM A36 steel in 1 M HCl. The PDP tests performed obtained polarization graph without and in presence of inhibitors as shown in Figure 2. The corrosion parameters based on extrapolated Taffel plots are shown in Table 2.

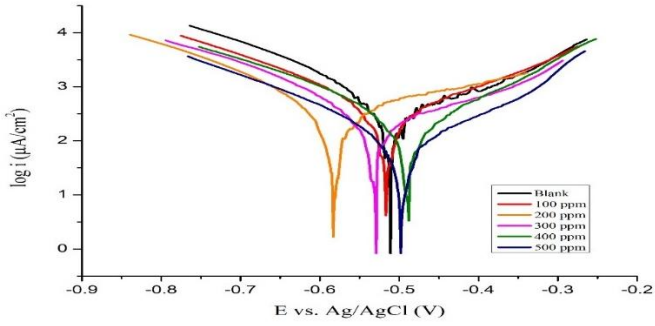

Figure 2. Potentiodynamic polarization curve for ASTM A36 Steel in 1 M HCl without and with various concentrations of inhibitors

Based on the Figure 2 that with the addition of inhibitors 100, 200, and 300 ppm, polarization curves

shifted to the cathodic direction. While with the addition of inhibitors 400 and 500 ppm the polarization curve shifts to the anodic direction. This shows that the addition of BCS extract causes the polarization of ASTM A36 steel with BCS extract inhibitors to shift irregularly. This irregularly is seen from the shift of the curve towards the cathodic and anodic direction affecting the cathodic and anodic constant as shown in Table 2. This occurs because the inhibitor affects anodic dissolution and cathodic hydrogen evolution, which indicates that BCS extract is mixed type (Gapsari et al., 2024). Chellouli et al. (2016), have previously reported that the use of BCS oil as a corrosion inhibitor on iron also showed mixed type behavior.

The addition of inhibitors to corrosive media is accompanied by the displacement of E_{corr} towards a more positive potential direction with increasing inhibitor concentration affecting cathodic and anodic behavior (Lashgari et al., 2021). The lower value of current density (i_{corr}) with the addition of inhibitor indicated that the inhibitor molecules can be adsorbed uniformly. The decreasing corrosion rate value with increasing inhibitor concentration indicates that there is a decrease in corrosion resistance as the inhibitor concentration increases (Hidayatullah et al., 2019). The shift of the corrosion rate to a lower value indicates that the cathodic and anodic reactions are significantly inhibited (Lgaz et al., 2020). Thus, the inhibition efficiency (IE) of BCS extract increases with increasing inhibitor concentration as shown in Table 2.

Table 2. Corrosion Parameters based on Extrapolation of Tafel Plots of ASTM A36 Steel

C (ppm)	βa (V/s)	-βc (V/s)	E_{corr} (V)	i_{corr} (μA/cm²)	C_R (mm/year)	IE (%)
Blank	0.102	-0.205	-0.511	255.59	5.958	-
100	0.108	-0.157	-0.517	204.36	4.764	20.04
200	0.089	-0.121	-0.583	149.97	3.496	41.32
300	0.091	-0.146	-0.529	122.57	2.857	52.04
400	0.085	-0.091	-0.488	86.82	2.024	66.03
500	0.086	-0.080	-0.498	40.22	0.937	84.26

EIS Measurement

Corrosion testing was also carried out using the EIS method. The results of EIS measurement show a Nyquist curve in the form of a semicircular diagram which is a plot of real impedance (Zr) and imaginary impedance (Zi) as shown in Figure 3. The shape of the Nyquist curve which perfectly forms a semicircle indicates that the surface of the test specimen is a homogeneous. The addition of the inhibitor shows that the diameter of the semicircular capacitance increases as the inhibitor concentration increases. Inhibitors are able to inhibit corrosion by enlarging the Nyquist curve along with the addition of corrosion inhibitors (Hadisaputra et al., 2019). The enlargement of the Nyquist curve is due to the increasing charge transfer resistance with the adsorption of inhibitor molecules (Doner et al., 2011).

The charge transfer resistance process plays a major role in increasing the adsorption surface coverage of inhibitor molecules on the ASTM A36 steel surface. The increased surface coverage of the adsorption of inhibitor molecules makes the inhibition efficiency value increase. This result is seen from the inhibitor charge transfer value (R_{ct}) as shown in Table 3. The EIS test results on ASTM A36 steel with the addition of corrosion inhibitor from BCS extract showed agreement with the potentiodynamic polarization (PDP) test. The inhibition efficiency value increases with increasing corrosion inhibitor concentration. Based on these results, BCS extract can act as a corrosion inhibitor for ASTM A36 steel.

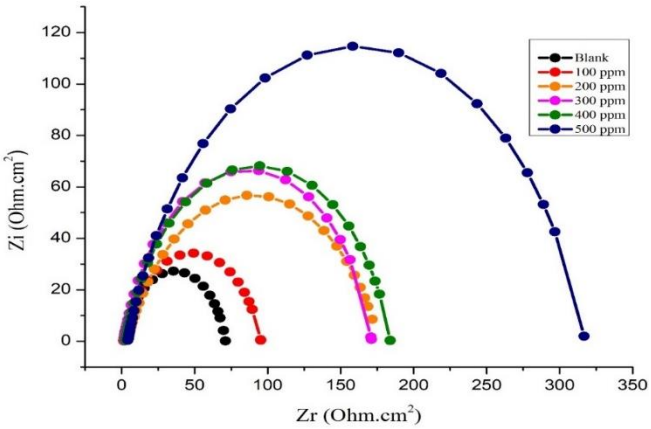

Figure 3. Nyquist curve of for ASTM A36 Steel in 1 M HCl without and with various concentrations of inhibitors

Table 3. Impedance Parameters for ASTM A36 Steel in 1 M HCl Solution without and with Various Concentrations of Inhibitors

C (ppm)	R_s (Ω.cm²)	R_{ct} (Ω.cm²)	CPE Y_o (×10⁻⁵S.sⁿ)	n	IE (%)
Blank	1.450	69.61	14.57	0.846	-
100	1.492	93.94	17.03	0.802	25.89
200	1.905	169.3	8.99	0.849	58.88
300	3.868	171.8	8.03	0.744	59.48
400	2.625	181.4	7.51	0.821	61.63
500	4.171	313.2	05.25	0.805	77.77

Adsorption Isotherm and Inhibition Explanation of BCS Extract

Adsorption of inhibitors on the surface of ASTM A36 steel can be shown by adsorption isotherms. Some equations used to calculate adsorption isotherms include Langmuir, Freundlich, Temkin, and Frumkin adsorption isotherms with equations 8 to 11, respectively (Gapsari et al., 2022):

$$\frac{C}{\theta} = \frac{1}{K_{ads}} + C \quad (8)$$

$$\log \theta = K_{ads} + n \log C \quad (9)$$

$$log \frac{\theta}{C} = log\, K_{ads} - a\theta \quad (10)$$

$$log \left\{\frac{\theta}{(1-\theta)C}\right\} = logK_{ads} + a\theta \quad (11)$$

with K_{ads} is the adsorption equilibrium constant, and a is a constant. Through this equation, plotting is carried out based on the linear regression equation, y= ax +b with b (intercept) is K_{ads}. Plotting to determine the adsorption isotherm is obtained with the best regression value (R^2). The adsorption isotherm based on plotting is Freundlich adsorption isotherm with R^2 is 0.98689 as shown at Figure 4. Determine of thermodynamic factors is done with the equation (Gapsari et al., 2024):

$$\Delta G°_{ads} = -RTln(55.5K_{ads}) \quad (12)$$

$$ln\, K_{ads} = \frac{-\Delta H°_{ads}}{RT} \quad (13)$$

$$\Delta G°_{ads} = \Delta H°_{ads} - T\Delta S°_{ads} \quad (14)$$

The values of the thermodynamic parameters are listed in Table 4. The $\Delta G°_{ads}$ value of about -20 kJ/mol or higher indicates electrostatic interaction (physisorption) and about -40 kJ/mol or lower involves charge transfer from the inhibitor to the metal surface forming a coordination bond (chemisorption) (Doner et al., 2016). Based on the $\Delta G°_{ads}$ value -10.971 kJ/mol, it is known that the BCS extract inhibitor is physisorption behavior. While the negative $\Delta H°_{ads}$ value indicates the adsorption process is exothermic and the positive $\Delta S°_{ads}$ value that the adsorption of the inhibitor takes place spontaneously forming a stable layer (El Hajjaji et al., 2016).

Table 4. Adsorption Parameters for BCS Extract on ASTM A36 Steel in 1 M HCl at 298 K

Isotherm Adsorption	K_{ads}	$\Delta G°_{ads}$ (kJ/mol)	$\Delta H°_{ads}$ (kJ/mol)	$\Delta S°_{ads}$ (kJ/mol.K)
Freundlich	1.51	-10.971	-1.021	0.033

Quantum Chemical Result

Figure 5 shows the electron distribution in the molecular orbitals of the major compounds of BCS methanol extract. Table 5 shown the quantum chemical parameters of mayor compounds of BCS extract are linoleic acid (LA), methyl linoleate (ML), 4-cyclopentene-1,3-dione,4-3-methyl-2-butenyl) (CP), methyl palmitate (MP), and palmitic acid (PA) as inhibitors.

Table 5. Quantum Chemical Parameters of Inhibitors with DFT B3LYP/6-31G(d)

Parameter	Inhibitors				
	LA	PA	CP	MP	ML
E_{HOMO} (eV)	-6.296	-7.438	-6.503	-7.288	-6.244
E_{LUMO} (eV)	0.334	0.342	-0.424	0.398	0.437
ΔE_{gab} (eV)	6.631	7.780	6.079	7.686	6.682
I (eV)	6.296	7.438	6.503	7.288	6.244
A (eV)	-0.334	-0.342	2.424	-0.398	-0.437
μ (Debye)	1.386	1.365	2.432	1.519	1.925
χ (eV)	2.981	3.547	4.464	3.445	2.903
η (eV)	3.315	3.890	2.039	3.843	3.341
σ (eV^{-1})	0.302	0.257	0.490	0.260	0.299
ΔN	0.277	0.163	0.087	0.178	0.287

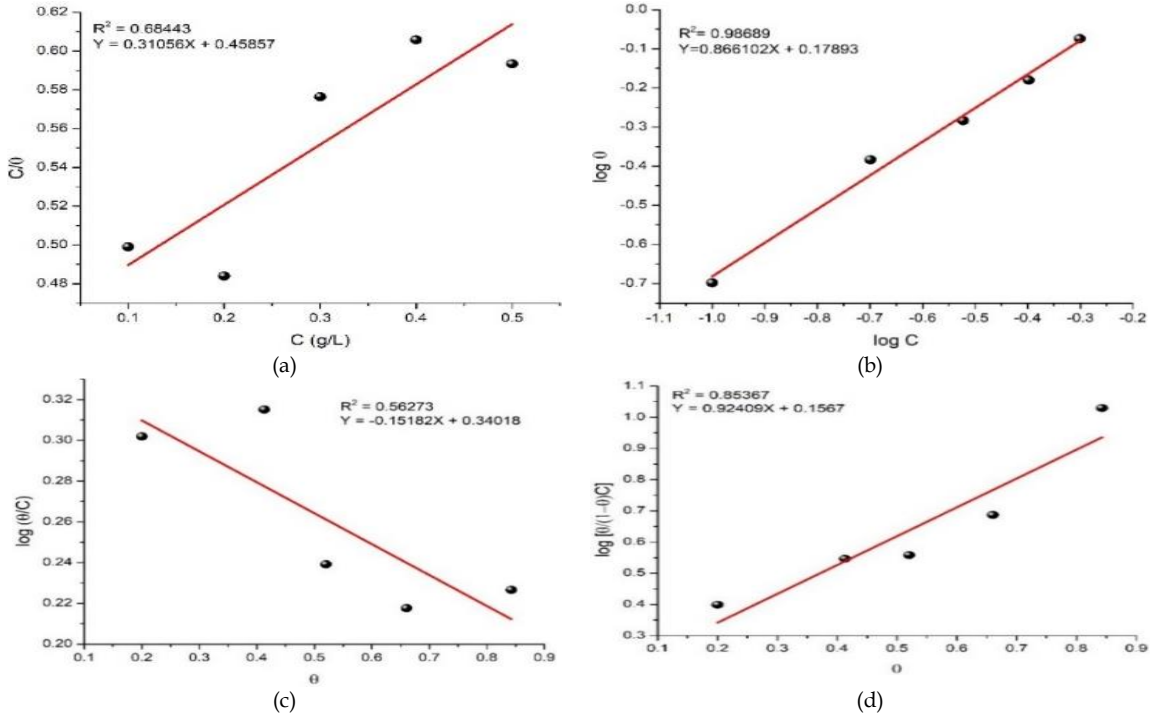

Figure 4. Adsorption isotherm fitting curves: (a) Langmuir, (b) Freundlich, (c) Temkin, (d) Frumkin

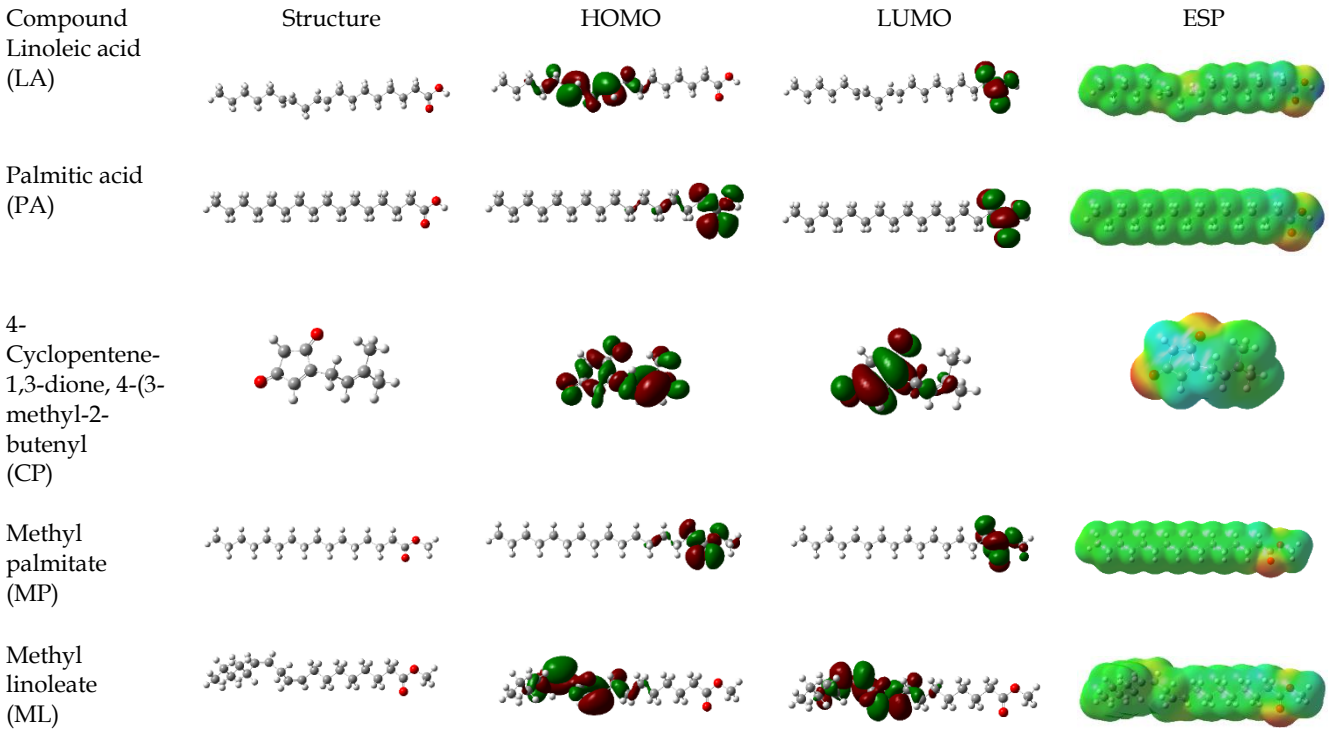

Figure 5. Visualization of the 2D structures, HOMO, LUMO, and ESP orbitals

Table 5 shown the values of quantum descriptor parameters including energy values of the highest occupied molecular orbital (E_{HOMO}) and the lowest unoccupied molecular orbital (E_{LUMO}), ΔE_{gab} (energy gab), ionization potential (IP), electron affinity (EA), electronegatifity (χ), hardness (η), softness (σ) and fraction of electrons transferred from the inhibitors to iron surface (ΔN). The values of this quantum descriptor parameters were obtained from the single point energy from running energy the DFT B3LYP/6-31G(d). The ability of inhibitors to donate electrons can be predicated by calculating the values of quantum descriptor parameters. E_{HOMO} is the energy that shows the ability of the inhibitor to donate its electrons to Fe metal (Hadisaputra et al., 2022). The value of E_{HOMO} will be directly proportional to the ability of the inhibitor to adhere to the metal surface.

Based on Table 1, the inhibitors that have the highest ability to contribute electrons when viewed from E_{HOMO} are ML > LA > CP > MP > PA. Based on the E_{HOMO} value, it can be predicate that the ML inhibitor in BCS extract has the greatest contribution in donating its electrons to Fe metal. Meanwhile, the ΔE_{gab} value is the ability of the inhibitor to adsorb on the metal. A high ΔE_{gab} value indicates low stability of the compound making it difficult to adsorb (Lgaz et al.,2020). Therefore, inhibitor compounds that have low ΔE_{gab} are able to adsorbed on metal surfaces more easily.

Table 5. Quantum Chemical Parameters of Inhibitors with DFT B3LYP/6-31G(d)

Parameter	Inhibitors				
	LA	PA	CP	MP	ML
E_{HOMO} (eV)	-6.296	-7.438	-6.503	-7.288	-6.244
E_{LUMO} (eV)	0.334	0.342	-0.424	0.398	0.437
ΔE_{gab} (eV)	6.631	7.780	6.079	7.686	6.682
I (eV)	6.296	7.438	6.503	7.288	6.244
A (eV)	-0.334	-0.342	2.424	-0.398	-0.437
μ (Debye)	1.386	1.365	2.432	1.519	1.925
χ (eV)	2.981	3.547	4.464	3.445	2.903
η (eV)	3.315	3.890	2.039	3.843	3.341
σ (eV^{-1})	0.302	0.257	0.490	0.260	0.299
ΔN	0.277	0.163	0.087	0.178	0.287

The value of electronegativity (χ) is related to the ability of compounds to flow electrons. Electrons will flow from low to high electronegativity (Hadisaputra et al., 2020). Compounds that have low electronegativity will more easily flow their electrons to Fe metal so that it is easy to adsorb on the metal surface. Table 5 shows that based on the electronegativity value, compounds ML >LA > MP > PA > CP are easily adsorbed on metal surfaces. While the electron transfer (ΔN) is interpreted as the ability of the electrons donated into the Fe surface, the more electrons will protect the Fe surface. The ability of compounds to donate electrons in the order of ML > LA > MP > PA > CP. This also corresponds to the value of electronegativity.

Monte Carlo Simulations

The interaction between inhibits, water molecules or corroding agents and metal surfaces can be seen in Monte Carlo (MC) simulations. MC simulation can predict the adsorption energy (total energy, adsorption energy, and deformation energy) to show the adsorption ability of the inhibitor on the Fe surface (Hsissou et al., 2020). Figure 6 shows the most stable adsorption pattern on the Fe(110) surface containing 100 molecules of water and 1 molecule of each inhibitor. The adsorption energy the inhibitor is much higher than the adsorption energy of water molecules as shown in Table 6. The adsorption energy with the largest negative value than the water adsorption energy indicates that the inhibitor can inhibit the adsorption of water that causes corrosion (Hadisaputra et al., 2022). Figure 6 shows that the adsorption of inhibitor molecules is in the position and condition most likely to be adsorbed on the Fe(110) surface. Jiang et al. (2018) stated that spatial structure of the compound when adsorbed has a great influence on the adsorption process.

Hadisaputra et al. (2021) state that the greater the negative value of molecular adsorption energy, the stronger the adsorption. Based on the adsorption value of each inhibitor on the Fe(110) surface, it can be seen that the compound molecules that have the strongest adsorption are ML> LA > PA > MP > CP. The adsorption ability of inhibitor compounds based on MC simulations is in line with the result of determining the quantum descriptor parameters of ML and LA compounds that have the greatest adsorption of each inhibitor is strong in the high value indicating that the adsorption of these inhibitor compounds is very good on the Fe metal surface. Based on the descriptor parameter value and Monte Carlo silulation, the results are well correlated. Hadisaputra et al. (2022) in their research also showed that the adsorption energy from MC simulation and quantum chemical parameters from DFT method have a good correlation.

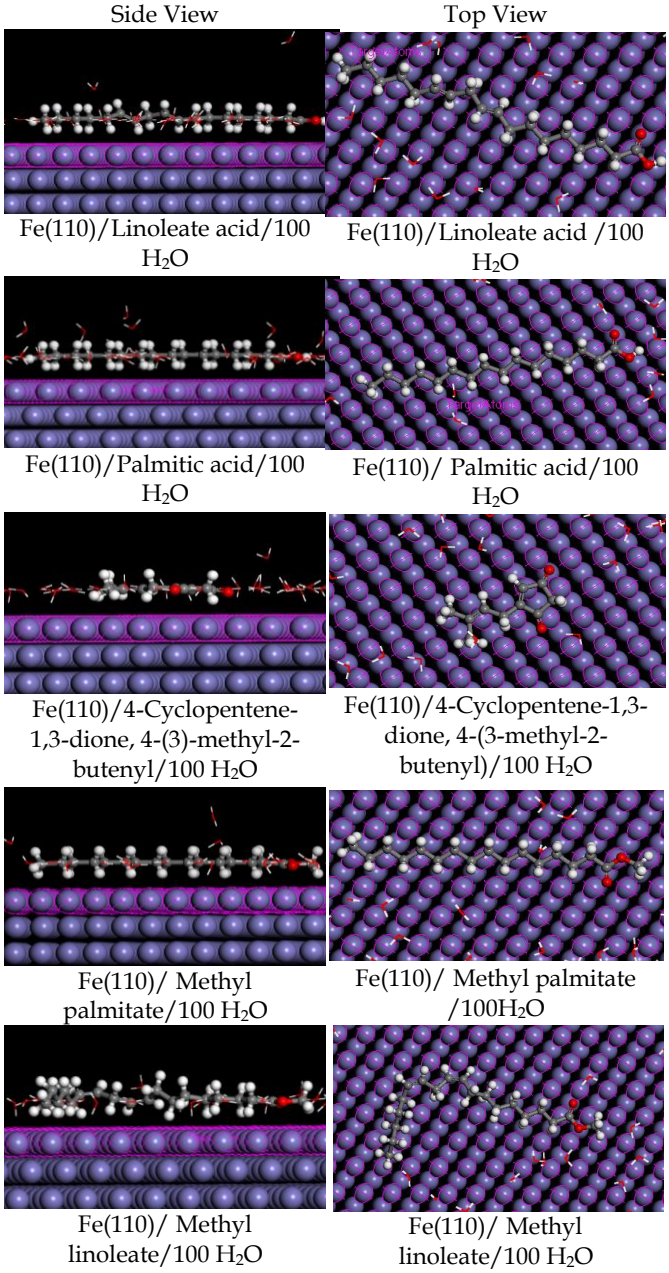

Figure 6. Adsorption of inhibitors on the surface of Fe(110) in the Monte Carlo simulation

Table 6. The Energy of Inhibitors Adsorption based on Monte Carlo Simulation

Inh	Adsorption Energy (Kcal mol^{-1})	Rigid Adsorption Energy (Kcal mol^{-1})	Deformation Energy (Kcal mol^{-1})	Inh: dE_{ad}/dN_i (Kcal mol^{-1})	H_2O: dE_{ad}/dN_i (Kcal mol^{-1})
LA	-4209.454	-1501.348	-2708.105	-198.746	-29.363
PA	-4144.152	-1430.121	-2714.031	-198.727	-29.899
CP	-4067.422	-1355.897	-2711.525	-118.202	-33.916
MP	-4228.485	-1521.548	-2706.937	-192.706	-29.577
ML	-4190.272	-1484.164	-2706.108	-207.0791	-30.130

Conclusion

The methanol extract of BCS (*Nigella sativa*) contains the major compounds are linoleic acid (25.12%), methyl linoleate (22.70%), 4-cyclopentene-1,3-dione,4-3-methyl-2-butenyl) (7.64%), methyl palmitate (6.66%), dan palmitic acid (5.14%). BCS extract in 1 M HCl solution showed corrosion inhibition on ASTM A36 steel. The PDP test results showed that the inhibition efficiency increased with increasing concentration. The

highest efficiency was 84.26% at 500 ppm inhibitor concentration. The results are in line with the EIS test, the inhibition efficiency increase with increasing concentration. The highest efficiency was 77.77% at 500 ppm inhibitor concentration. Computational studies were used to know the adsorption and role of major compounds in BCS extract. The strongest inhibit compound was ML (methyl linoleate) based on quantum descriptor parameter study and MC simulation.

Author Contributions

Conceptualization, S. H.; methodology, Y. M.; software, Y. M.; validation, S. H., S.H. and S.; formal analysis, Y.M.; investigation, S.H.; resources, S.H.; data curation, Y.M.; writing—original draft preparation, Y.M.; writing—review and editing, Y.M.; visualization, S.H.; supervision, X.X.; project administration, S.H. All authors have read and agreed to the published version of the manuscript.

Funding

This research received no external funding.

Conflicts of Interest

The authors declare no conflict of interest.

References

Alrashidi, M., Derawi, D., Salimon, J., & Yusoff, F.(2020). An Investigation of Physicochemical Preperties of Nigella sativa L. Seed Oil from Al-Qassim by Different Extraction Methods. *Journal of King Saud University-Science*. https://doi.org/10.1016/j.jksus.2020.09.019

Chellouli, M., Chebabe, D., Dermaj, A., Erramli, H., Bettach, N., Hajjaji, N., Casaletto, M. P., Cirrincione, C., Privitera, A., & Srhiri, A. (2016). Corrosion Inhibition of Iron in Acidic Solution by a Green Formulation Derived from Nigella sativa L, *Electrochimica Acta*, *204*, 50–59. https://doi.org/10.1016/j.electacta.2016.04.015

Döner, A., Solmaz, R., Özcan, M., & Kardaş, G. (2011). Experimental and Theoretical Studies of Thiazoles as Corrosion Inhibitors for Mild Steel in Sulphuric Acid Solution, *Corrosion Science*, *53*(9), 2902–2913. https://doi.org/10.1016/j.corsci.2011.05.02

El Hajjaji, F., Greche, H., Taleb, M., Chetouani, A., Aouniti, A., & Hammouti, B. (2016) Application of Essential Oil of Thyme vulgaris as Green Corrosion Inhibitor for Mild Steel in 1 MHCl, *Journal of Materials and Environmental Science*, *7*(2), 567–578.

Gapsari, F., Setyarini, P. H., Kurniawan, F., Ahnaf, A., Anwar, M. S., & Zuryati, U. S. (2022). Corrosion Inhibition of Weldment by Nephelium lappaceum Peel Extract in 3.5% NaCl Solution. *South African Journal of Chemical Engineering*, 41, 223-232. https://doi.org/10.1006/j.sajce.2022.06.006.

Gapsari, F., Styarini, P. H., Utariningrum, F., Sulaiman, A M., Haidar, M. F., & Julian, T. S. (2024). Melaleuca Leaves Extract as Eco-Friendly Inhibitor for Low carbon Steel in Sulfuric Acid. *Case Studies in Chemical and Environment Engineering*, 9, 100657. https://doi.org/10/1016/j.cscee.2024.100657.

H., K., L., A., & M., M. (2018). Comparative Assessment of Extraction Methods and Quantitative Estimation of Thymoquinone in The Seeds of Nigella sativa L By HPLC, *International Journal of Pharmacognosy and Phytochemical Research*, *9*(12), 1425–1428. https://doi.org/10.25258/phyto.v9i12.11186

Hadisaputra, S., Hamdiani, S., Kurniawan, M. A., & Nuryono, N. (2017). Influence of Macrocyclic Ring Size on The Corrosion Inhibition Efficiency of Dibenzo Crown Ether: A Density Functional Study, *Indonesian Journal of Chemistry*, *17*(3), 431–438. https://doi.org/10.22146/ijc.26667

Hadisaputra, S., Purwoko, A. A., & Hamdiani, S. (2022). Copper Corrosion Protection by 4-Hydrocoumarin Derivatives: Insight from Density Functional Theory, Ab Initio, and Monte Carlo Simulation Studies, *Indonesian Journal of Chemistry*, *22*(2), 413–428. https://doi.org/10.22146/ijc.69530

Hadisaputra, S., Purwoko, A. A., Rahmawati, Asnawati, D., Ilhamsyah, Hamdiani, S., & Nuryono. (2019). Experimental and Theoretical Studies of (2R)-5-hydroxy-7-methoxy-2-phenyl-2,3-dihydrochromen-4-one as Corrosion Inhibitor for Iron in Hydrochloric Acid, *International Journal of Electrochemical Science*, *14*, 11110–11121. https://doi.org/10.20964/2019.12.77

Hadisaputra, S., Purwoko, A. A., Savalas, L. R. T., Prasetyo, N., Yuanita, E., dan Hamdiani, S. (2020). Quantum Chemical and Monte Carlo Simulation Studies on Inhibition Performance of Caffeine and Its Derivatives Against Corrosion of Copper, *Coatings*, *10*(11), 1–17. https://doi.org/10.3390/coatings10111086

Hassan, H., Ismail, A., Ahmad., S., & Soon, C. F. (2017). Super-Hydrophobic Corrosion Inhibitor on Carbon Steel, *Materials Science and Enginering*, 215, 1-5.

Hidayatullah, S., Gapsari, F., & Setyarini, P. H. (2019). ASTM A36 Iron Corrosion Behavior in Hydrochloric Acid (HCl) with Fish Scale Chitosan Inhibitor. *National Seminar on Innovation and Application of Technology in Industry*

Hsissou, R., Abbout, S., Seghiri, R., Rehioui, M., Berisha, A., Erramli, H., Assouag, M., & Elharfi, A. (2020). Evaluation of Corrosion Inhibition Performance of Phosphorus Polymer for Carbon Steel in [1 M] HCl: Computational Studies (DFT, MC and MD

simulations), *Journal of Materials Research and Technology*, *9*(3), 2691–2703. https://doi.org/10.1016/j.jmrt.2020.01.002

Jiang, L., Qiang, Y., Lei, Z., Wang, J., Qin, Z., & Xiang, B. (2018). Excellent Corrosion Inhibition Performance of Novel Quinoline Derivatives on Mild Steel in HCl Media: Experimental and Computational Investigations, *Journal of Molecular Liquids*, *255*(2017), 53–63. https://doi.org/10.1016/j.molliq.2018.01.133

Kabir, Y., Akasaka-Hashimoto, Y., Kubota, K., & Komai, M. (2020). Volatile Compounds of Black Cumin (Nigella sativa L.) Seeds Cultivated in Bangladesh and India, *Heliyon*, *6*(10), e05343. https://doi.org/10.1016/j.heliyon.2020.e05343

Kardas, G., & Yazıcı, B. (2014). *Electrochemical and Quantum Chemical Studies of 2-amino-4-methyl-thiazole as Corrosion Inhibitor for Mild Steel in HCl Solution*. https://doi.org/10.1016/j.corsci.2014.02.029

Lashgari, S. M., Bahlakeh, G., & Ramezanzadeh, B. (2021). Detailed Theoretical DFT Computation/Molecular Simulation and Electrochemical Extrapolations of Thymus vulgaris Leave Extract for Effective Mild-Steel Corrosion Retardation in HCl Solution. *Journal of Molecular Liquids*, 335, 115897. https://doi.org/10.1016/j.molliq.2021.115897

Lgaz, H., Chung, I. M., Albayati, M. R., Chaouiki, A., Salghi, R., & Mohamed, S. K. (2020). Improved Corrosion Resistance of Mild Steel in Acidic Solution by Hydrazone Derivatives: An Experimental and Computational Study, *Arabian Journal of Chemistry*, *13*(1), 2934–2954. https://doi.org/10.1016/j.arabjc.2018.08.004

Mulyati, B., Si, S., & Si, M. (2019), *Tanin dapat Dimanfaatkan sebagai Inhibitor Korosi*.

Obot, I. B., Solomon, M. M., Umoren, S. A., Suleiman, R., Elanany, M., Alanazi, N. M., & Sorour, A. A. (2019). Progress in The Development of Sour Corrosion Inhibitors: Past, Present, and Future Perspectives, *Journal of Industrial and Engineering Chemistry*, *79*, 1–18. https://doi.org/10.1016/j.jiec.2019.06.046

Prasad, A. R., Kunyankandy, A., & Joseph, A. (2020). Corrosion Inhibition in Oil and Gas Industry: Economic Considerations, *Corrosion Inhibitors in The Oil and Gas Industry*, 135–150. https://doi.org/10.1002/9783527822140.ch5

Salarvand, Z., Amirnasr, M., Talebian, M., Raeissi, K., & Meghdadi, S. (2017). Enhanced Corrosion Resistance of Mild Steel in 1 M HCl Solution by Trace amount of 2-phenyl-benzothiazole Derivatives: Experimental, Quantum Chemical Calculations and Molecular Dynamics (MD) Simulation Studies, In *Corrosion Science* (Vol. 114). Elsevier Ltd. https://doi.org/10.1016/j.corsci.2016.11.002

Saleh, M. M., Mahmoud, M. G., & El-Lateef, H. M. (2019). Comparative Study of Synergistic Inhibition of Mild Steel and Pure Iron by 1-hexadecylpyridium Chloride and Bromide Ions. *Corrosion Science*, 154, 70-79. https://doi.org/10.1016/j.corsci.2019.03.048

Samal, P. P., Singh, C. P., & Krishnamurty, S. (2023). Expounnding Lemonal Terpenoids as Corrosion Inhibitors for Copper Using DFT Based Calculations, *Journal Applied Surface Science*, 614, 156066